

PAPER • OPEN ACCESS

Magneto-rheological dampers—model influence on the semi-active suspension performance

To cite this article: Juan C Tudon-Martinez *et al* 2019 *Smart Mater. Struct.* **28** 105030

View the [article online](#) for updates and enhancements.

You may also like

- [Physics-enhanced neural networks for equation-of-state calculations](#)
Timothy J Callow, Jan Nikl, Eli Kraiser et al.
- [An automated, quantitative, and case-specific evaluation of deformable image registration in computed tomography images](#)
R G J Kierkels, L A den Otter, E W Korevaar et al.
- [Direct voltage control of magnetorheological damper for vehicle suspensions](#)
Haiping Du, James Lam, K C Cheung et al.



ECS
The
Electrochemical
Society
Advancing solid state &
electrochemical science & technology

DISCOVER
how sustainability
intersects with
electrochemistry & solid
state science research

Magneto-rheological dampers—model influence on the semi-active suspension performance

Juan C Tudon-Martinez¹ , Diana Hernandez-Alcantara¹ ,
Luis Amezquita-Brooks², Ruben Morales-Menendez³,
Jorge de J Lozoya-Santos³  and Osvaldo Aquines¹

¹ Universidad de Monterrey, Av. Morones Prieto 4500, 66238, San Pedro Garza García NL, México

² UANL, Av. Universidad s/n, 66450, San Nicolás de los Garza N.L., México

³ Tecnológico de Monterrey, Av. Garza Sada 2501, 64849, Monterrey N.L., México

E-mail: juan.tudon@udem.edu

Received 9 June 2019, revised 17 July 2019

Accepted for publication 9 August 2019

Published 5 September 2019



CrossMark

Abstract

Recently, automotive industry has adopted semi-active damper systems to improve handling and comfort properties of vehicles. Nowadays, *Magneto-Rheological (MR)* dampers are among the most effective solutions; with the control algorithm used for their operation being a key element. While basic controllers do not require mathematical damper models, improved performance can be achieved if these are available. Usually, the accuracy of a particular set of models can be assessed by evaluating standard quantitative metrics. However, two models with similar error-metrics can still have widely different qualitative properties. In this context, the main aim of this paper is to study the effects that may appear in the closed-loop performance of an automotive suspension system when the damper model is unable to represent crucial nonlinear *MR* phenomena. To highlight the model influence on the controller synthesis and subsequently on the suspension performance, two damper models with different accuracy levels were chosen: an *Artificial Neural Networks (ANN)*-based model is compared with the classical *Bingham* model. First, their accuracy is experimentally validated using typical error-metrics. Afterwards, the same suspension control strategy is designed using both models. *Frequency-Estimation-Based* control was selected because it better exploits available model data than other typical strategies such as *sky-hook*. The resulting performance is assessed with a *software-in-the-loop* approach using *CarSim*[®] and complemented with a *hardware-in-the-loop* implementation using a *CAN-bus*, both closed-loop control cases use a *Simulation-Oriented ANN* model as benchmark to represent the *MR* damper nonlinearities. Results show that although the difference in error-metrics between models can be small using typical identification methods (e.g. 16% in one scenario), suspension performance in comfort and road-holding are significantly different. Error-metrics can be deceptive for assessing the effectiveness of *MR* damper models during the controller design phase. Accurate qualitative modeling in the pre/post-yield regions are the main factors which determine the resulting controller performance.

Keywords: magneto-rheological damper, semi-active suspension control, vehicle suspension

(Some figures may appear in colour only in the online journal)

 Original content from this work may be used under the terms of the [Creative Commons Attribution 3.0 licence](https://creativecommons.org/licenses/by/3.0/). Any further distribution of this work must maintain attribution to the author(s) and the title of the work, journal citation and DOI.

1. Introduction

Vehicle manufacturers are constantly trying to improve security and riding comfort. One of the key components

involved in this process is the vehicle suspension. The main function of dampers is to dissipate the kinetic energy, reducing the motion of the sprung mass (i.e. vehicle chassis) and improving the road-holding. While it is possible to adjust the suspension elements passively by mechanical design, it has been shown that active or semi-active systems can improve performance (Dixon 2007, Savaresi et al 2010, Fijalkowski 2011). In this regard, active elements are capable of inducing arbitrary forces to provide the best performance; however, they have higher energy requirements and a complex mechanical implementation (Fijalkowski 2011). On the other hand, semi-active dampers allow modifying the dynamical properties of the suspension system with less energy consumption and mechanical complexity. The result is that semi-active systems are less expensive, yielding a better level of performance-versus-cost ratio (Savaresi et al 2010). In this context, *Magneto-Rheological (MR)* dampers present several attractive properties such as: low power requirement, fast response, simple structure and a wide range of adjustable damping coefficient (Dixon 2007).

In addition to an adequate actuator, semi-active suspension systems require control algorithms capable of managing the dissipativity and saturation constraints of the damper to improve the desired handling and ride-comfort properties. Several *Automotive Suspension Control Systems (ASCS)* have been proposed with varying levels of success. For some of these proposals an accurate damper model is unnecessary. For example, the well known *sky-hook* and *ground-hook* controllers only require data of the suspension deflection velocity and sprung or unsprung mass velocity instead of a complete damper model. On the other hand, better knowledge of the physical system can be used to improve the performance. That is, if an accurate damper model is available then model-based control strategies can be used to achieve better results. Examples of these control schemes can be found in (Do et al 2012, Poussot-Vassal et al 2012), where *Linear Parameter-Varying (LPV)* systems are used to consider the model-based actuator constraints for a robust controller design.

In *MR* dampers, the rheological properties of the fluid are modified by the magnetic field generated by a coil located within the damper, according to a time-varying electrical current signal. This allows modifying the properties of the vehicle suspension on-line. However, the actual relationship between the electric current and the resulting damping force is highly nonlinear. *MR* dampers, unlike passive ones, present variable average damping coefficients, hysteresis loops and saturation levels (Dutta and Chakraborty 2015). Moreover, other dynamical phenomena such as friction, viscous damping and yield stress have also been detected when time-varying electric currents are considered (Lozoya-Santos et al 2012). Indeed, in a typical closed loop control operation where the *MR* damper current is modified on-line, additional dynamical modes are also introduced. This discussion highlights the difficulties in obtaining proper *MR* damper models. For this purpose two major approaches have been proposed in the literature: structured and non-structured models.

Structured models are comprised by mathematical representations with a predefined structure. This approach

allows relating particular model parameters to specific physical behaviors. For instance, the yield stress phenomenon could be related to a particular parameter. Examples of these models are the classical *Bingham* model (Stanway et al 1987), the *Bouc–Wen* models (Spencer et al 1996, Werely et al 1998, Yang et al 2002, Dutta and Chakraborty 2014, Waubke and Kasess 2016) and the algebraic models proposed in (Guo et al 2006, Kwok et al 2006, Çesmeçi and Engin 2010, Singru et al 2017). The *Bouc–Wen* and the algebraic models aim to represent common nonlinearities with high accuracy. However, these models suffer from having too many parameters, some of them related with the internal structure of the damper. Therefore, they can be difficult to characterize experimentally. Among structured models, the *Bingham* model is capable of reproducing variable damping coefficient, saturation and hysteresis with a simple structure; making this model attractive for practical applications.

Non-structured models are mainly data-based, yielding gray or black box-type representations. Examples of this approach, based on techniques such as *Artificial Neural Networks (ANN)*, fuzzy logic, statistical inference and polynomial approximations, can be found in (Choi et al 2001, Chang and Zhou 2002, Hong et al 2002, Guo et al 2004, Du et al 2005, 2006, Savaresi et al 2005, Zapateiro et al 2009, Metered et al 2010, Boada et al 2011, Tudón-Martínez et al 2012, Imaduddin et al 2017, Tang et al 2017). The main advantage of these models is the possibility of achieving very high levels of accuracy at the cost of losing the physical interpretation of the model parameters. Among these techniques, *ANN*-based modeling yields simpler structures because the decoupling of the jounce/rebound effects of the damper is not necessary. In addition, it has been observed that *ANN* models have good extrapolation properties, simpler identification algorithms and it is possible to achieve a low number of model parameters (Tudón-Martínez et al 2012) when the *ANN* design is based on the minimal dimensions criterion. This is relevant because simpler *ANN* models have low computational overhead and are suitable for practical applications. In contrast, if a very high level of accuracy is required, a complex *ANN* can be used by introducing recurrent architectures, redundant inputs, time delayed input vectors and/or increment of the network size at the cost of higher computational overhead. An interesting study about the trade-off between complexity and modeling accuracy using an *ANN* is presented in (Tudón-Martínez et al 2012).

Due to the particular characteristics of structured and non-structured models their utilization for the design of closed loop control systems differs. In particular, inverse dynamics-based control is the most representative approach used with non-structured models, particularly with *ANN* (Chang and Zhou 2002, Savaresi et al 2005, Zapateiro et al 2009, Metered et al 2010, Boada et al 2011). Other control-oriented problems considering *ANN* are presented in (Guo et al 2004, Imaduddin et al 2017); usually *ANN*-based models are very attractive to add fault-tolerance to the suspension control systems. On the other hand, structured models are especially suitable for analytical design methods, such as those based on *LPV* systems (Do et al 2012, Poussot-Vassal et al 2012).

The previous discussion shows that a direct comparison between the actual effectiveness of structured and non-structured models can be difficult since the controller design approaches used for each are different. In this regard, some research projects have presented interesting comparative studies among models (Song *et al* 2005, Şahin *et al* 2010, Sandu *et al* 2010, Wang and Song 2011, Tudón-Martínez *et al* 2012). These reports assess the models in terms of key features such as model error, number of parameters, complexity, processing time, identification methods, etc. However, these studies only highlight the resulting model properties, but not their actual usefulness for designing effective control systems. In this sense, the main contribution of this paper is to present a qualitative and quantitative analysis of the effects that can occur in the closed-loop control performance of an automotive suspension system when the damper model, used for the controller design, is simple or has limitations to represent all nonlinear *MR* phenomena.

To clarify this situation consider that two models, *A* and *B*, have been assessed quantitatively using the *Root Mean Square (rms)* error, achieving both a similar level of accuracy. However, assume that it has been observed that model *A* is able to predict the hysteresis properties while model *B* is better at predicting force saturation. If the same control design method is applied with both models it would be valid to wonder which would yield the best performance. Moreover, it is not clear which model would be better for particular control objectives, maybe model *A* is better for improving comfort and model *B* for road-holding. These aspects are important if the very best performance is required. In this regard it is important to note that in current literature it is common to propose suspension controllers without considering the actual behavior of the damper, i.e. dissipativity, saturation, friction, etc (Karnopp *et al* 1974, Valasek *et al* 1997, Hong *et al* 2002). In fact, it is typical to assume that an arbitrary force can be exerted by the semi-active damper, which is contrary to the dissipative nature of the device (Savaresi *et al* 2005).

The previous discussion highlights the necessity of studying further the relationship between particular model properties and the resulting effectiveness for control design. In this article this problem is explored by first assessing the quantitative and qualitative accuracy of two models: the well known *Bingham* damper model and a simple *ANN* model. Some researches have demonstrated that *Bingham* model is a simple model, which is quick and practical while *ANN*-based model is more precise; however, their resulting effectiveness for control design is not clear, e.g. it is unknown which model is better for designing a comfort-oriented controller. Thus, the main purpose of this paper is to qualitatively and quantitatively analyze the effects of damper model accuracy in the controller design. Particularly, to determine the impact on the suspension performance (comfort and road-holding) when the damper model used during the controller design is unable to represent the typical *MR* phenomena in the pre-yield and post-yield stress regions, such the stiffness, friction, nonlinear viscoelasticity and hysteresis.

The control strategy applied to both models allows extracting all the relevant frequency domain information contained in

Table 1. Definition of variables.

Variable	Description	Units
c_0	Viscous damping coefficient in the <i>Bingham</i> model	N s m^{-1}
f_0	Preloaded damping force in the <i>Bingham</i> model	N
f_c	Dynamic yield force in the <i>Bingham</i> model	N A^{-1}
F_{MR}	<i>MR</i> damper force	N
I	Electric current	A
k_i	Time delays in a <i>NARX</i> model	—
k_s	Spring stiffness coefficient	N m^{-1}
k_t	Wheel stiffness coefficient	N m^{-1}
m_s	Sprung mass in the <i>QoV</i>	kg
m_{us}	Unsprung mass in the <i>QoV</i>	kg
z_{def}	Damper piston position	m
\dot{z}_{def}	Damper piston velocity	m s^{-1}
z_r	Road profile	m
z_s	Vertical position of m_s	m
\dot{z}_s	Vertical velocity of m_s	m s^{-1}
\ddot{z}_s	Vertical acceleration of m_s	m s^{-2}
z_{us}	Vertical position of m_{us}	m
\dot{z}_{us}	Vertical velocity of m_{us}	m s^{-1}
\ddot{z}_{us}	Vertical acceleration of m_{us}	m s^{-2}

the design models, which has been shown to be the main aspect which defines the dynamics of suspension systems. The resulting controllers (one based on the *Bingham* model and other on *ANN*) are then implemented using a *Software-in-the-Loop (SiL)* solution with the *CarSim*[®] simulator. To represent the *MR* damper dynamics in a very accurate representation of the complete vehicle suspension system, a *Simulation-Oriented ANN (SO-ANN)* model is used in this *SiL* environment. The *SO-ANN* model, in comparison with the *Bingham* and simple *ANN* models, has such a high level of accuracy, both quantitatively and qualitatively, that it can be used as a benchmark of the behavior of the *MR* damper. Thus, the *SO-ANN* model, which mimics with high accuracy the *MR* damper behavior, allows comparing the closed-loop suspension performance that is achieved using each damper model (*Bingham* or simple *ANN*) during the controller design. This comparative analysis is carried-out in time and frequency domains to yield useful conclusions.

Finally, the difficulty of implementing complex control algorithms is a limitation for practical applications. To explore this aspect, the considered controller (designed using the *Bingham* model and *ANN* model) is implemented in a *Hardware-in-the-Loop (HiL)* configuration using a low power micro-controller and considering a networked operation using a *Controller Area Network (CAN)*. The most used variables in this paper are defined in table 1, and the abbreviations are described in table 2.

2. *MR* damper modeling

The behavior of automotive dampers is typically assessed through their *Force-Velocity (FV)* diagram. Figure 1 shows the typical *FV* diagram of an *MR* damper under sinusoidal

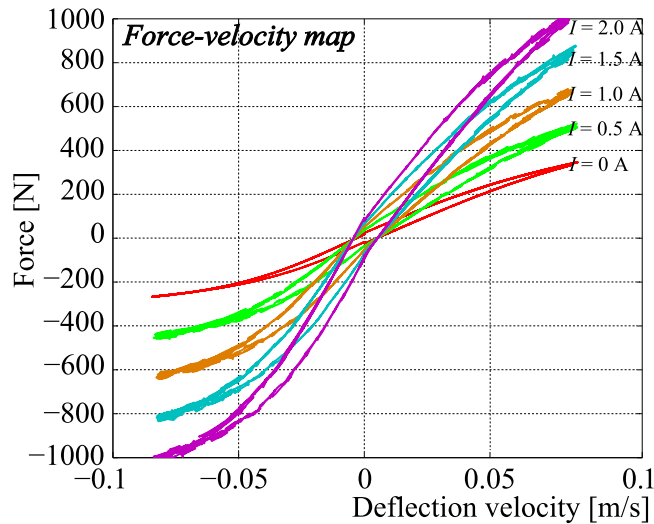


Figure 1. Nonlinear behavior of an MR damper.

Table 2. Description of acronyms.

Acronym	Description
AM	Amplitude-Modulated
ANN	Artificial Neural Networks
ASCS	Automotive Suspension Control Systems
BSS	Bounce Sine Sweep
CAN	Controller Area Network
DAQ	Data Acquisition System
DoE	Design of Experiments
ECU	Electronic Control Unit
FB	Frequency Band
FEB	Frequency-Estimation-Based
FM	Frequency-Modulated
FV	Force-Velocity
HiL	Hardware-in-the-Loop
ICPS	Increased Clock Period Signal
K&C	Kinematics and Compliance
LPV	Linear Parameter-Varying
MLP	Multi-Layer Perceptron
MR	Magneto-Rheological
NARX	Nonlinear Autoregressive eXogenous
QoV	Quarter of Vehicle
rms	Root Mean Square
RP	ISO Road Profile
SC	Stepped increments
SFS	Stepped Frequency Sinusoidal
SiL	Software-in-the-Loop
SO-ANN	Simulation-Oriented ANN
TPNVS	Triangular wave with Positive and Negative Variable Slopes

excitation considering different electric current inputs. This figure confirms that MR dampers present variable average damping coefficients, hysteresis and saturation.

There are several approaches which have been proposed to model MR dampers. The typical approach for model assessment consists in comparing the force of a given set of models with the real force obtained from an experimental setup. Using this method both quantitative and qualitative

considerations can be made. Examples of this approach can be found in (Song et al 2005, Şahin et al 2010, Sandu et al 2010, Wang and Song 2011, Tudón-Martínez et al 2012).

On the other hand, the *effectiveness* of a given model can be defined as how useful the model in question is for a particular application, such as mechanical design, controller design, simulation accuracy, performance testing, etc (Lozoya-Santos et al 2012). In the context of ASCS, the ultimate purpose of MR damper models is to design appropriate control algorithms. In this sense, the most *effective* model for ASCS is that which yields the best control algorithm. This article explores the evaluation of MR damper models taking into account this notion.

The first model considered is the well-known *Bingham* model (Stanway et al 1987), which has a parametric structure aimed at modeling the hysteresis FV loops, especially at high frequencies. This model comprehends a *Coulomb* friction element placed in parallel with a viscous damper and assumes that the fluid remains rigid in the pre-yield region. In the post-yield region, it considers a linear relation between the damping and deformation rate (Stanway et al 1987). The resulting damper force considering the *Bingham* model is given by:

$$F_{MR}(t) = f_0 + I(t) \cdot f_c \cdot \text{sign}[\dot{z}_{def}(t)] + c_0 \cdot \dot{z}_{def}(t), \quad (1)$$

where f_0 is the preloaded damping force, f_c is the dynamic yield force, c_0 is the viscous damping coefficient, I is the electric current and \dot{z}_{def} is the relative velocity of extension/compression of the damper rod, i.e. the damper deflection velocity.

For the comparison a simple non-structured model is proposed, in this case an ANN-based model. One complication which arises when using non-structured models is the difficulty of knowing *a priori* which particular configuration (i.e. number of neurones, input variables, etc) will render the best results for a particular application. For instance, if the model is aimed at simulation accuracy then more complex structures will be required at the cost of computational overhead. On the other hand, for control design a good balance of model accuracy and complexity is preferred. That is, for ASCS applications a slight loss of accuracy is permissible if a markedly simpler model is available. In most cases this balance has to be explored through direct experimentation.

In (Tudón-Martínez et al 2012), the main features of ANN-based MR damper models are studied comprehensively. This study revealed, that suspension deflection velocity and electric current are the main variables required for accurate modeling. This reduces the necessity of including redundant input variables, such as in (Chang and Zhou 2002, Savaresi et al 2005, Du et al 2006). In addition, time delayed inputs, as those proposed in (Chang and Zhou 2002, Savaresi et al 2005, Zapateiro et al 2009), are less important if an appropriate sampling time is used. Particularly, a sample time in the range of 3 ms was found to be effective. Finally, the model accuracy can be improved by introducing recurrent ANNs, as supported by the findings reported in (Chang and Zhou 2002, Savaresi et al 2005, Du et al 2006, Chen et al 2009, Zapateiro et al 2009, Metered et al 2010). These ANNs have been found to be effective for modeling complex nonlinear dynamical phenomena. However, in (Tudón-Martínez et al 2012) it was

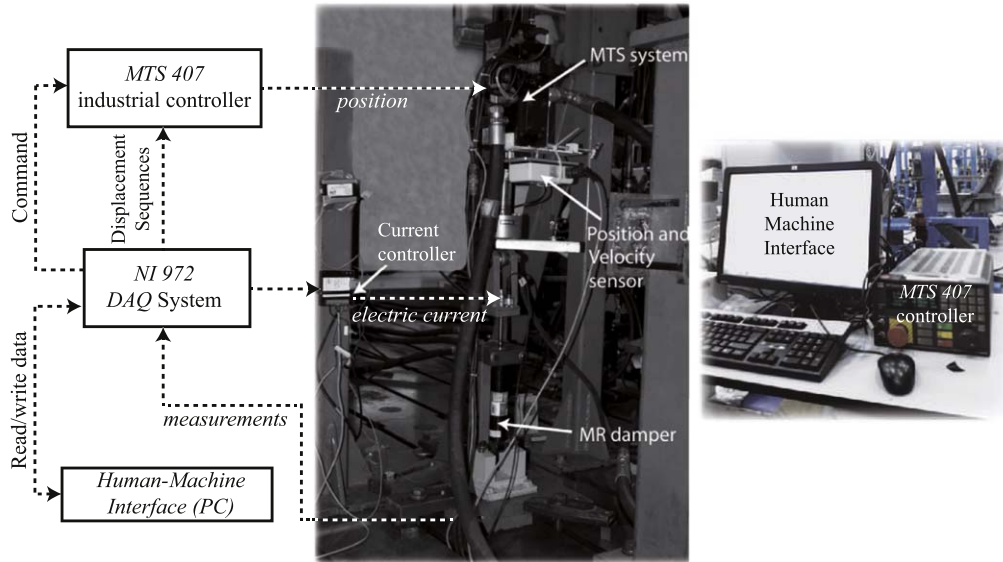


Figure 2. Experimental system.

found that linear accuracy improvements when using recurrent ANNs translate to exponentially increasing computing times. Therefore, it is recommended to limit the use of recurrent ANNs to applications where accuracy is more important than model complexity.

In this article feedforward ANNs are preferred over other variants because their learning algorithms do not require complex computational operations and it is not necessary to know the initial values of the parameters. MR damper models have been obtained using Radial Basis-Function networks, but these networks have the drawback of requiring a pre-clustering step which complicates the training process (Du *et al* 2006).

The extensive study presented in (Tudón-Martínez *et al* 2012) shows that an ANN-based model with a simple feedforward *Multi-Layer Perceptron* (MLP) structure is capable of representing two different commercial MR dampers with good accuracy, while keeping the model simple enough to be used in real-time control applications. Considering an MLP architecture as (L_i, L_m, L_o) with L_i , L_m and L_o neurones in the input, middle and output layers respectively, the ANN structure (2, 10, 1) has shown in (Tudón-Martínez *et al* 2012) to be appropriate for MR damper modeling and can be treated as the following nonlinear mapping of the damper deflection velocity $\dot{z}_{def}(t)$ and the electric current input $I(t)$ to the resulting damper force:

$$F_{MR}(t) = f(\dot{z}_{def}(t), I(t)). \quad (2)$$

In this article a *SiL* arrangement (described in section 4.1) is used to evaluate the resulting closed loop performance through the *CarSim*[®] simulator. This approach has the advantage of including the complete vehicle dynamics; however, it requires a highly accurate model to represent the actual MR damper. Therefore, an additional ANN model, oriented to simulation accuracy, is also introduced. In comparison to models (1) and (2), which are used for controller design and are intended to be simple, this model can be as complex as required. After extensive testing it was determined that excellent model accuracy

could be achieved for the MR damper studied in this article using a recurrent ANN with a (4, 10, 1) structure, a recurrent feedback of 2 delayed samples of the damping force, a delayed sample of the inputs and a sampling time of 0.625 ms. The general mathematical representation of this model is shown next:

$$\begin{aligned} F_{MR}(k) = f(z_{def}(k), z_{def}(k-1), z_{def}(k-2), \\ \dot{z}_{def}(k), \dot{z}_{def}(k-1), \dot{z}_{def}(k-2), \\ I(k), I(k-1), I(k-2), F_{MR}(k-1), F_{MR}(k-2)). \end{aligned} \quad (3)$$

In addition to having a more complex internal structure than model (2), this *SO-ANN* model (3) has a recurrent structure which allows modeling highly nonlinear dynamics. This characteristic is important because it has been observed that in practice MR dampers do have an important dynamical component (Şahin *et al* 2010, Sandu *et al* 2010, Lozoya-Santos *et al* 2012).

In the following section the experimental characterization of a real MR damper using the *Bingham* model (1), the ANN model (2) and the *SO-ANN* model (3) is presented.

2.1. Experimental characterization of an MR damper

In this section a commercial MR damper manufactured by *Delphi MagneRide*[™] is characterized using the test bench shown in figure 2. This damper allows using a continuous input signal, has a stroke of 40 mm, time constant of 15 ms and force range of ± 4000 N. On the other hand, the test bench comprises an hydraulic actuator of 15 kN at 2068 kPa with a stroke of 0.06 m, an *MTS-407*[™] controller and a *NI-9172*[™] DAQ which measures the relevant variables with a sampling frequency of 1650 Hz.

Appropriate excitation of the electric current $I(t)$ and the damper deflection $z_{def}(t)$ are required in order to properly characterize key nonlinearities of the semi-active damper. In particular, steady state sinusoidal excitation of the damper

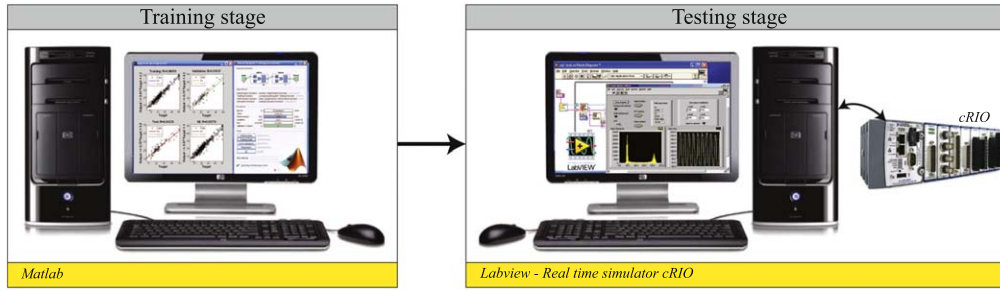


Figure 3. Procedures to train and test an MR damper model.

Table 3. DoE to identify an MR damper. Displacement sequences: TPNVS, Triangular wave with Positive and Negative Variable Slopes; SFS, Stepped Frequency Sinusoidal; RP, ISO Road Profile; AM, Amplitude-Modulated; and FM, Frequency-Modulated. Electric current sequences: SC, Stepped inCrements; and ICPS, Increased Clock Period Signal, (Lozoya-Santos et al 2012).

Experiment	Displacement sequence	Current sequence	Analyzed dynamics
E_1	TPNVS A ^a : 17.8 mm F ^b : [0.5–15] Hz	SC 10 steps: 0, 0.25, ..., 2.5 A	Dynamic behavior at constant velocity and different electric current values.
E_2	SFS A: 12.7 mm F: [0.5–15] Hz	SC 10 steps: 0, 0.25, ..., 2.5 A	Hysteresis loops in the frequency range of interest at different electric current values.
E_3	RP type D A: 25 mm F: [0.5–3] Hz	ICPS [0–2.5] A	Typical vehicle suspension motion at standard road conditions (ISO 8608).
E_4	AM A: [0–25] mm F: 2.8 Hz	ICPS [0–2.5] A	Transient response of MR force around to the natural frequency of m_s at variable road roughness.
E_5	FM A: 25 mm F: [0.5–15] Hz	ICPS [0–2.5] A	Hysteresis loops at different frequencies by adding the nonlinear transient effects of the actuation.

^a Absolute amplitude of the displacement sequence.

^b Frequency of the displacement sequence.

deflection with constant values of $I(t)$ is not sufficient for adequate characterization of the hysteresis loops and nonlinear transient responses of the damping force (Du et al 2006, Chen et al 2009, Boada et al 2011). In (Lozoya-Santos et al 2012) an experimental methodology designed specifically for MR damper characterization was proposed. According with this methodology, table 3 shows the *Design of Experiments (DoE)* used in this article. Some of the main features of the DoE are displacement and electric current ranges of ± 25 mm and 0–2.5 A, respectively, with a displacement bandwidth between 0.5 and 15 Hz. This bandwidth is enough for evaluating comfort and road holding in automotive applications.

2.2. Modeling results

In order to validate the capabilities of models (1)–(3) to represent the dynamical behavior of the commercial MR damper, different replicas of the experiments described in table 3 have been used. In order to assess the resulting performance of each model the following index, based on the

rms error, is used:

$$\text{Error (\%)} = \frac{\sqrt{\left(\sum_{i=1}^n [F_{MR}(i) - \hat{F}_{MR}(i)]^2\right)}}{\sqrt{n} \cdot \max_{\forall i \in n} F_{MR}} \times 100\%, \quad (4)$$

where $\hat{F}_{MR}(\cdot)$ and $F_{MR}(\cdot)$ represent the estimated and experimental damping force, respectively, and n is the number samples in the experiment.

The Bingham model was identified by using a nonlinear least squares method based on the L^2 -norm of the modeling error, while the ANN-based models were trained with the Levenberg–Marquardt algorithm.

Figure 3 shows the setup used in the training and testing stages. Matlab[®] was used to compute and execute the learning algorithms. On the other hand, the testing procedure was carried out in a National InstrumentsTM cRIO 9014 real time simulator using a sampling rate of 200 Hz.

Each experiment was repeated ten times to improve the validity of the results. In each experiment 60% of the data obtained was used for model identification and the remainder for evaluating the model performance. Figure 4 illustrates the flowchart of the modeling procedure in general. The model

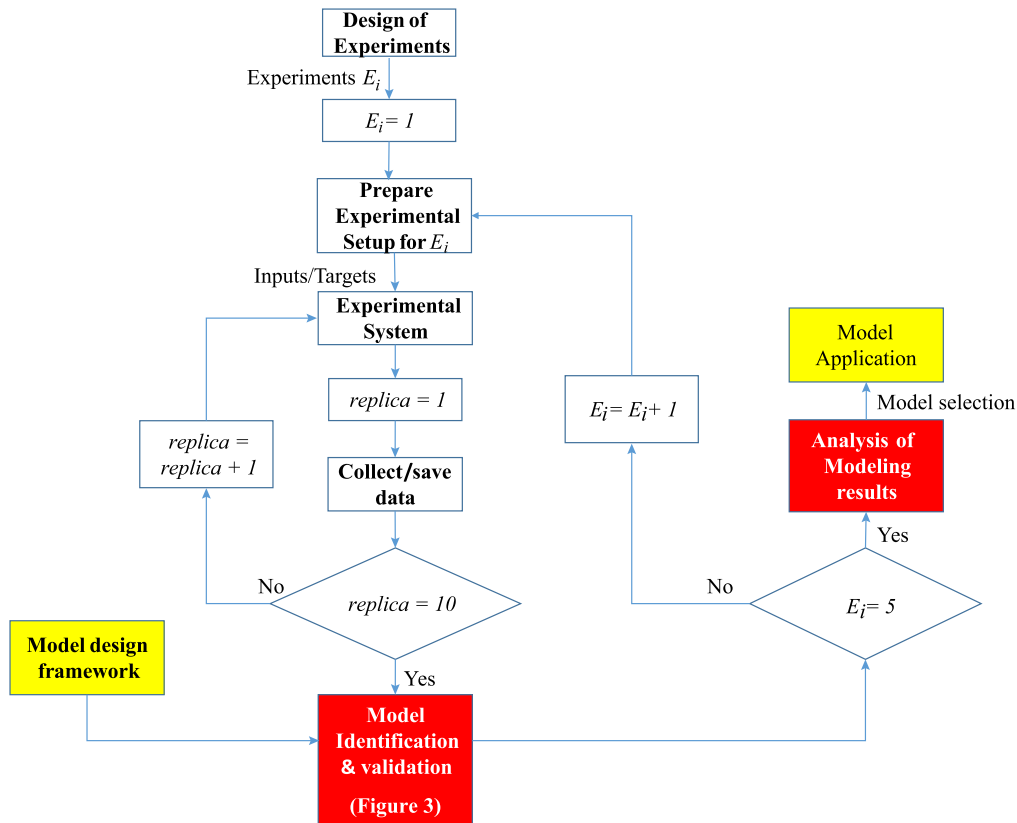


Figure 4. Block diagram of the modeling procedure.

Table 4. Modeling error with the control-oriented models and simulation-oriented model.

Model	Error (%)					Statistical indexes	
	E_1	E_2	E_3	E_4	E_5	Mean	Std. Deviation
<i>Bingham</i>	8.9	16.6	19.1	17.4	17.9	16.0	4.1
<i>ANN</i>	5.9	8.4	3.0	4.0	14.9	7.2	4.8
<i>SO-ANN</i>	1.7	7.0	1.6	3.8	3.0	3.4	2.2

design framework (control or simulation oriented) follows the operation dynamics of interest according to (Lozoya-Santos *et al* 2012); while, the architecture of the *ANN*-based models is based on the minimal dimensions criterion discussed in (Tudón-Martínez *et al* 2012). The analysis of the modeling results has been carried out in quantitative and qualitative form, using the *rms* error and *FV* curve respectively. The selection of the identified model parameters (*Bingham* or *ANN*-based model) for control purposes depend on the vehicle dynamics required to test in a closed-loop operating condition.

Table 4 shows the quantitative resulting performance of each model in the five experiments. A comparison of the mean modeling error of all the experiments of table 3 reveals that the *ANN*-based model has an improvement of 55% compared with the *Bingham* model; whereas the simulation-oriented model (i.e. *SO-ANN*) has the lowest error level, with a mean error 52% lower than the control-oriented *ANN* model.

On the other hand, the results show that there are important differences in modeling error depending on the experiment. For instance, in experiment E_3 an improvement of 84% can be obtained using the *ANN* model instead of the *Bingham* model; however, in experiment E_5 the difference is only 16%. In comparison, the *SO-ANN* model presented an improvement of 79% over the *ANN* model for the same experiment. Finally, the typical damper identification method is given by experiment E_1 showing a difference of 33% in the modeling error between the *ANN* and *Bingham* models, which is a moderate error level.

The previous discussion confirms the notion that model accuracy is dependent on the experimental conditions. Therefore, it is difficult to know the effectiveness of each model for a particular task by assessing the model error quantitatively. That is, an indirect evaluation of the *model-effectiveness* through a quantitative error index is difficult without further knowledge. For example, intuition indicates that if the conditions of experiment E_5 are more relevant than

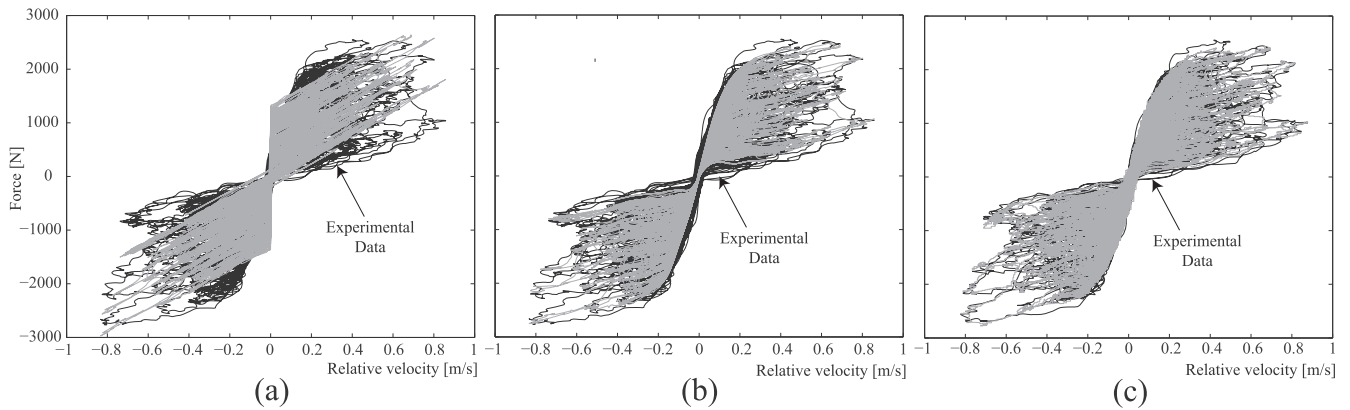


Figure 5. *FV* diagram for different *MR* damper models, experiment E_3 (Tudón-Martínez et al 2012): (a) control-oriented *Bingham* model, (b) control-oriented *ANN*-based model, (c) simulation-oriented *ANN*-based model.

those of E_3 for controller design then the *ANN*-based model will be only marginally more effective than the *Bingham* model for this purpose. In this case only a much more complex representation, such as the *SO-ANN* model, with its recurrent structure and low error across all conditions, would introduce significant improvements. Conversely, if the conditions of experiment E_3 are more relevant than those of E_5 then *ANN*-based model will be more effective for a controller design in comparison to the *Bingham* model. In the next section a direct evaluation of the effectiveness of each model will be presented by designing and implementing model-based closed loop controllers.

A more thorough qualitative assessment of each model for one experiment is presented next. Although more involved, this kind of comparisons can reveal deeper nuances that quantitative error indexes cannot. For instance, figure 5 compares the *FV* diagram obtained for each model based on the same experimental data (E_3 , road profile). Clearly, the *SO-ANN* model shows the best modeling performance and is able to represent the effects of jounce and rebound when the electric current changes. In comparison, the control-oriented *ANN* model has some limitations to fit the nonlinearities at low relative velocities. Nonetheless, in general it correctly captures the dependency between viscous damping coefficient and electric current. On the other hand, some clear modeling drawbacks are exhibited with the *Bingham* model: (a) in the post-yield region, the viscous damping effect is linear, (b) the pre-yield region is narrower than the experimental one, inducing an overestimation of the resulting force around $\dot{z}_{def} < 0.1 \text{ m s}^{-1}$, and (c) the force does not saturate at high velocities, showing instead a linear *FV* proportionality. Additionally, since the *Bingham* model assumes symmetry between the jounce and rebound effects, the compression force cannot be well represented for asymmetric dampers (Tudón-Martínez et al 2012). Similar qualitative results were obtained with the other experimental conditions of table 3.

In summary, the qualitative model assessment revealed that the *Bingham* model has problems to correctly predict: (a) the hysteresis *FV* loops at higher frequencies observed in experiments E_1 , E_2 and E_5 , (b) the friction phenomenon produced when there is a change of sign in the position, e.g.

in experiments E_1 , E_2 and E_5 , (c) the nonlinear viscous damping in the pre and post-yield region seen in experiments, E_1 , E_3 and E_4 , and (d) the saturation effect in all experiments.

Finally, a novel complementary experiment was performed to evaluate the extrapolation properties of the models. This experiment is comprised by a displacement *SFS* with an exponentially decreasing amplitude (from 12.7 to 1 mm) accompanied with a *SC* sequence for the electric current. In this case, the *Bingham* model showed an error of 15.1%, the *ANN*-based model 2.7% and the *SO-ANN* model 1.5%.

3. Modeling effect on the suspension controller design

The main objective of this section is to analyze the modeling effects of an *MR* damper into the design of a semi-active suspension controller; allowing to ascertain the relationship between the model properties obtained in the last section with the actual effectiveness of each model for controller design.

In model-based control an accurate model is required if high-performance operation is desired. This follows from the fact that if a high degree of model uncertainty is expected then the robustness margins need to be increased during the design stage. This normally results in a more conservative controller, which will typically yield a lower performance (Choi et al 2002, Wang et al 2005, Poussot-Vassal et al 2008, Chadli et al 2010). On the other hand, if a very low level of model uncertainty is considered then a more aggressive control strategy could potentially yield a higher level of performance. Examples of this dependency can be found in several control strategies such as the classical *sky-hook* or *ground-hook* approaches with the damping coefficient (Karnopp et al 1974, Valasek et al 1997, Lozoya-Santos et al 2011) or with the best damping combination in (Tudon-Martinez et al 2018).

In this context it could be argued that an *optimal MR* damper model (for controller design) will be that which allows designing high-performance model-based controllers, regardless of the level of model accuracy reported by any particular quantitative measure (Prabakar et al 2014). In the last section it was shown that the *ANN* was, by most

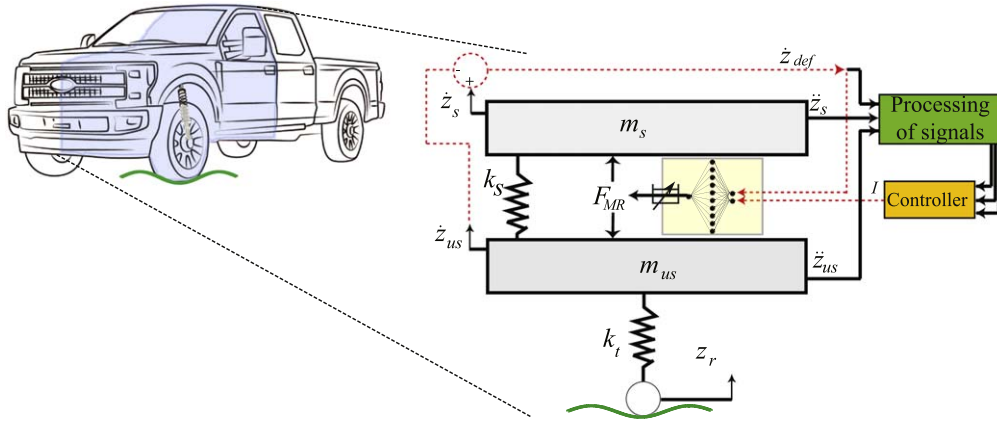


Figure 6. General structure of a *QoV* semi-active suspension control system. In this case, the *MR* force is represented by an *ANN*-based model.

measures, a more accurate model than the *Bingham* model. Using these models as case of study, high-performance semi-active suspension controllers are designed to elucidate how well model accuracy translates to the resulting controller performance.

According to the previous modeling results, experiment E_1 explores the main nonlinear *MR* phenomena in the frequency band (FB) of interest. Thus, the identified parameters of the *Bingham* and *ANN* model with this data-set were chosen for the controller synthesis (i.e. in the *Model Application* block in figure 4).

Since the control strategy used for the comparison is based on a decentralized *QoV* topology its corresponding model is presented next. A *QoV* can be represented by a sprung mass (m_s) and an unsprung mass (m_{us}). A linear spring with stiffness coefficient k_s and an *MR* damper represent the suspension between both masses. The stiffness coefficient k_t models the wheel tire. The vertical position of the mass m_s (m_{us}) is defined by z_s (z_{us}), while z_r corresponds to the road surface. It is assumed that the wheel-road contact is ensured. The system dynamics is given by:

$$\begin{aligned} m_s \ddot{z}_s &= -k_s(z_s - z_{us}) - F_{MR} \\ m_{us} \ddot{z}_{us} &= k_s(z_s - z_{us}) - k_t(z_{us} - z_r) + F_{MR}, \end{aligned} \quad (5)$$

where, F_{MR} is the *MR* damper force calculated with either the *Bingham* or the *ANN*-based models. The *QoV* model parameters described in equation (5) have been identified from a commercial pickup truck, table 5.

The *Frequency Estimation-Based (FEB)* control approach proposed in (Lozoya-Santos *et al* 2011) was selected to analyze the effects of the *MR* damper model in the controller design. The *FEB* control algorithm is given by:

$$F_{MR} = \begin{cases} F_{soft}(I_{min}) & \hat{f} \in \{FB_1, FB_2, \dots, FB_i\} \\ F_{hard}(I_{max}) & \text{otherwise} \end{cases}, \quad (6)$$

where the *MR* damping force is soft/hard at the minimum/maximum actuation (electric current), and \hat{f} is the on-line estimated frequency of the suspension motion. In this case, the design task consists of determining the FBs FB_i according

Table 5. *QoV* model parameters of a pickup truck.

Front <i>QoV</i>		Rear <i>QoV</i>	
Parameter	Value	Parameter	Value
m_s	630 (kg)	m_s	387 (kg)
m_{us}	81.5 (kg)	m_{us}	139.5 (kg)
k_s	42 500 (N m ⁻¹)	k_s	37 300 (N m ⁻¹)
k_t	230 000 (N m ⁻¹)	k_t	230 000 (N m ⁻¹)

to the desired suspension performance in the frequency domain (Lozoya-Santos *et al* 2011).

Figure 6 shows a conceptual diagram of a *QoV* semi-active suspension control system using the *FEB* controllers. In order to calculate the *MR* damper force either model (i.e. *ANN* or *Bingham*) can be used. These models use the suspension deflection velocity and electric current to estimate the *MR* damper force. On the other hand, the *FEB* controller uses measurements and/or estimations of the suspension motion to calculate the frequency response of the *QoV* suspension system and determine the optimal current level for all the possible vehicle conditions, creating a look-up table. The look-up table definition can be performed off-line or on-line if improved damper model data are available. A *signal processing* module is used to estimate in a short time-window the frequency content of the *QoV* motion as described in (Tudon-Martinez *et al* 2015). This data is used on-line by the controller module to select the optimal electric current for the *MR* damper according to the specified comfort and/or road holding performance.

The main feature of the *FEB* control approach is its high dependency on the *MR* damper model. In particular, the model is used to determine the proper damping coefficient required to reduce the chassis motion and wheel vibrations according with the main frequency content of the measured variables. During this process no model uncertainty is considered. As such, this approach is akin to a direct model cancellation, rendering it particularly sensitive to its accuracy.

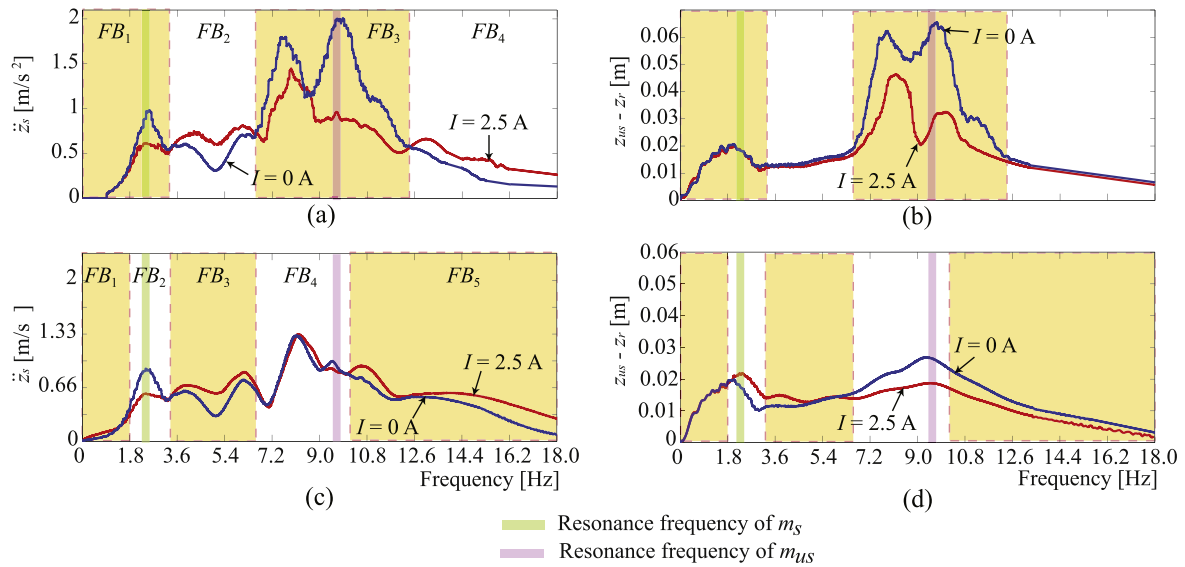


Figure 7. Frequency response in a front *QoV* model dynamics: (a) sprung mass acceleration using the ANN-based damper model, (b) tire deflection using the ANN-based damper model, (c) sprung mass acceleration using the *Bingham* model, (d) Tire deflection using the *Bingham* model.

This renders the *FEB* control scheme a good candidate to evaluate model effectiveness for control design.

Figure 7 represents the frequency responses of a frontal *QoV* when the ANN and *Bingham* models are used to represent the semi-active damping force. The sprung mass acceleration is related with the comfort performance while the tire deflection evaluates the road holding. In all cases the frequency responses are presented in two conditions, when the electric current of the MR damper is 2.5 A and 0 A, respectively. This allows assessing the bounds of the comfort and road-holding corresponding to the maximum and minimum damping force that can be exerted by the MR damper. The main differences in the frequency responses of each model are discussed as follows:

- Around the resonance frequency of m_{us} (~ 9 Hz):
 - Note in figure 7(c) that the *Bingham* model shows an almost invariant sprung mass acceleration with respect to the damper current, while the ANN model predicts a much wider gain difference, figure 7(a).
 - In the case of the tire deflection the gain is around 200% larger in the ANN model response, figures 7(b) and (d). This larger magnitude obtained with the ANN-based model is caused by a better semi-activeness property in the actuator model, and thanks to the good capability of the ANN to represent nonlinearities at high frequencies.
- The previous observations indicate that a comfort-oriented controller designed with the *Bingham* model will tend to predict much lower improvements by operating the damper with a higher current level than a controller designed with the ANN model. This difference will have an important effect when deciding whether a high or low level of current is used for the damper.
- Around the resonance frequency of the sprung mass (~ 2 Hz):
 - The *Bingham* model shows a trade-off between comfort and road holding because the sprung mass acceleration is reduced with the maximum damping

Table 6. Look-up tables of the *FEB* suspension controllers considering (a) the ANN-based damper model or (b) the *Bingham* model for a front corner of a pickup truck.

(a) ANN-based model					
	FB_1	FB_2	FB_3	FB_4	
Frequency (Hz)	0–3.2	3.2–6.6	6.6–12.2	>12.2	
Electric current (A)	2.5	0	2.5	0	

(b) <i>Bingham</i> model					
	FB_1	FB_2	FB_3	FB_4	FB_5
Frequency (Hz)	0–1.8	1.8–3.2	3.2–6.0	6.0–10.0	>10.0
Electric current (A)	0	trade-off	0	2.5	trade-off

force while the tire deflection is minimized with the minimum damping force. This trade-off is not present with the ANN-based damper model.

The previous discussion highlights key differences in the behavior predicted by each model in the most relevant FBs for this application. As follows it will be shown that these differences are effectively translated into the controller tuning parameters. According with the tuning method described in (Lozoya-Santos *et al* 2011) *FEB* controllers were synthesized with each model; resulting in the look-up tables summarized in table 6. It is clear that the resulting *FB* configuration is different when using each model.

The process was repeated for each vehicle corner, resulting in similar differences in the look-up tables of the corresponding *FEB* controllers.

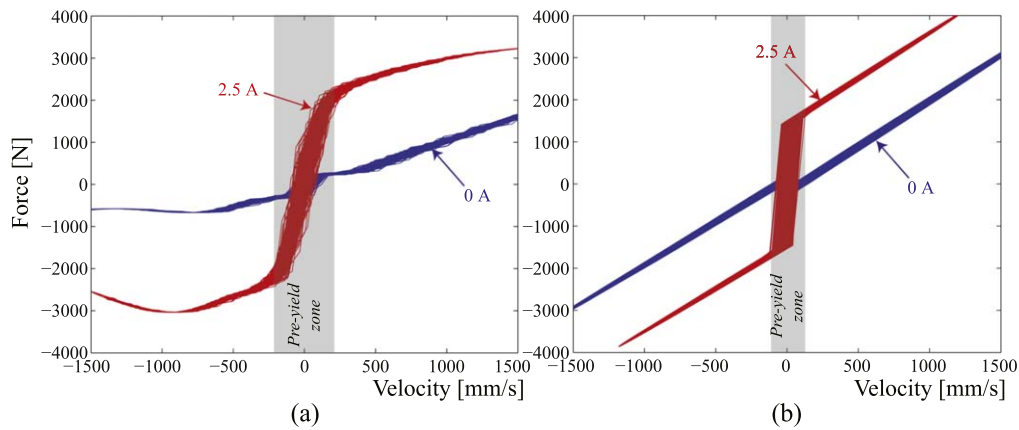


Figure 8. *FV* diagrams of both *MR* damper models in an automotive suspension open-loop control system: (a) *ANN* model, (b) *Bingham* model. A sinusoidal signal is considered as road input in the *QoV* model.

Finally, the main focus of this article is to present the effects of damper model choice for high-performance model-based control, such as the *FEB* scheme. Nonetheless, the following paragraph presents a complementary discussion which considers the damping coefficient bounds, denoted as c_{min} and c_{max} . These parameters are used for controller tuning by more traditional schemes such as the *sky-hook* approach. In order to estimate c_{min} and c_{max} it is common to calculate the damper *FV* diagrams considering both high and low currents. Figure 8 shows the *FV* diagrams of both *MR* damper models. In figure 8 it can be observed that the pre-yield zone in the *ANN*-based model is wider, i.e. the friction phenomenon is present in a larger range of suspension deflection velocity. On the other hand, the viscous damping (the slope in the post-yield zone) is higher in the *Bingham* model, e.g. at 1.2 m s^{-1} the force in the *ANN*-based model (@ 2.5 A) is around 3000 N while in the *Bingham* model is around 4000 N. Similarly, this inconsistency occurs in the curve at 0 A. From figure 8 it is clear that the resulting c_{min} and c_{max} will be markedly different with each model.

4. Modeling effect on the suspension control performance

In the previous sections it was shown that different semi-active damper models yield distinct *ASCS* behaviors and accordingly different controllers when using a model-based control scheme. In this section the effects of these differences will be explored further. The objective is to extend the notion of semi-active damper *model accuracy* into that of *model effectiveness* for model-based control applications. In particular, two studies were performed:

- (i) A *SiL* simulation by using the *CarSim*[®] software. The vehicle simulator has a suspension control system configuration of independent corners, i.e. each wheel-station has an *MR* damper with an independent *FEB* controller. In this simulation study, the most accurate *SO-ANN* model in equation (3) is used as benchmark to

evaluate the suspension control performance obtained with the controllers designed using models (1) and (2).

- (ii) An experimental *HiL* platform based on a *CAN* network. This setup allows evaluating the resulting controllers in a more realistic environment subject to noise and other perturbations. The complete *QoV* system (considering the *SO-ANN* damper model) is embedded in a real-time industrial controller to mimic the suspension phenomena as close as possible, whereas the control algorithm is hosted in a low cost micro-controller. A *CAN* bus keeps the communication between the two devices such as in commercial cars. This process includes converting the control and actuator signals into the analog domain before digital reacquisition and *CAN* bus communication in order to inject more realistic noise and perturbations.

4.1. Analysis in the *CarSim*[®] simulator

The vehicle model used to evaluate the influence of the *MR* damper model into the automotive suspension system was characterized from experimental data obtained from a *K&C* (*Kinematics and Compliance*) test over a commercial vehicle (pickup truck of medium payload). A *CarSim*[®] generic pickup model was customized for the particular vehicle considered in this study using *K&C* data. The customization of the suspension system is mainly composed of the physical dimensions (weight, longitude, width, height, wheel base, front and rear track, etc), kinematics real data curves (camber angles, dive angles, caster angles, damping force, jounce/rebound stops, spring and tire stiffness, etc), structural parameters (mechanical ratios, compliance coefficients, Kingpin geometry, etc) and compliance of the suspension system (independent wheel stations at the front side and a rear solid axle at the back). Figure 9 illustrates some parameters of the vehicle model, whose kerb weight is around 2000 kg, as well as some experimental nonlinear curves introduced in *CarSim*[®] for the kinematics and compliance of the front and rear suspension system.

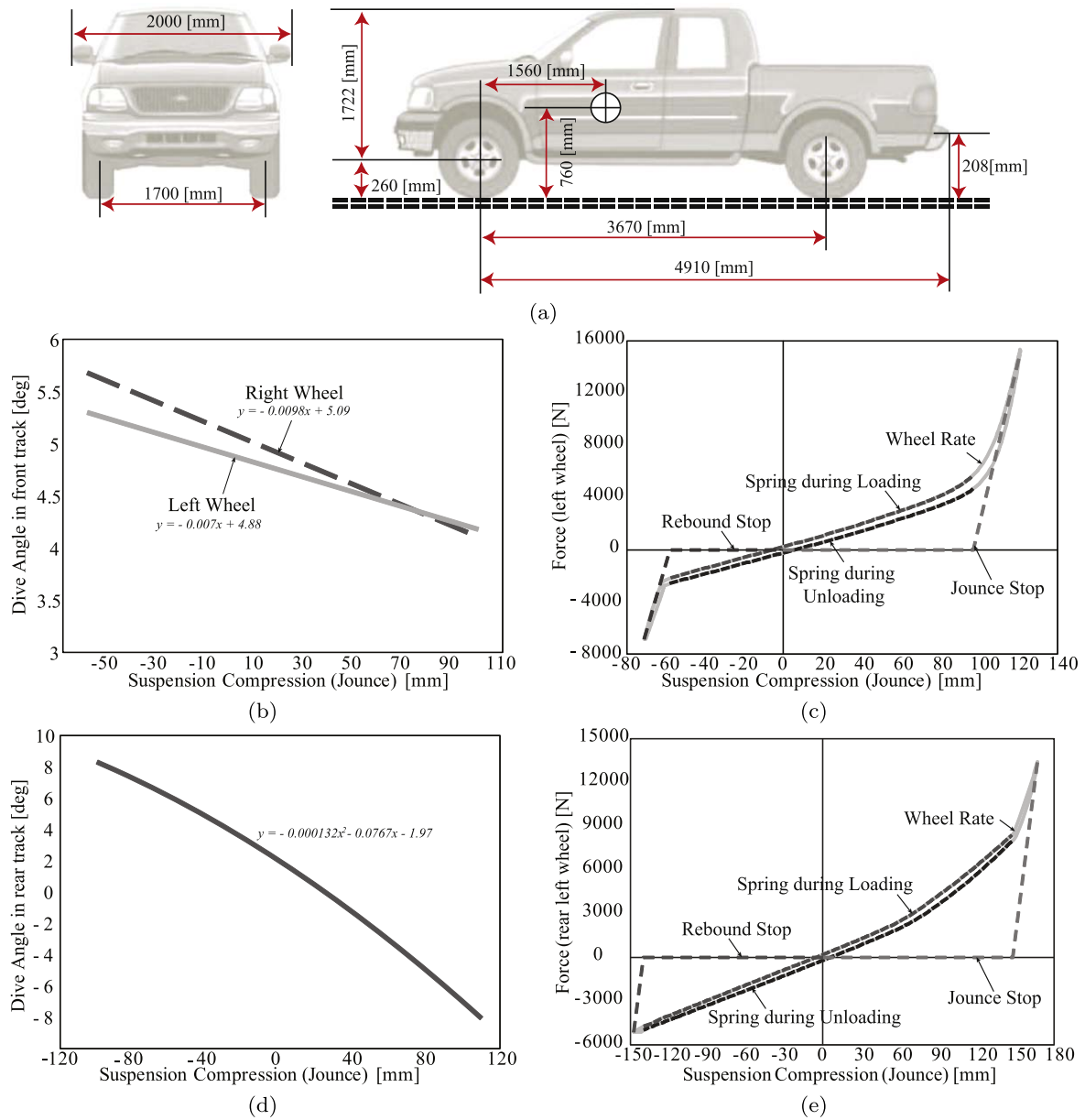


Figure 9. Some parameters and nonlinear curves to characterize the kinematics and compliance of a medium-payload vehicle model customized in *CarSim*[®].

Although each corner is independently controlled, the global load transfer is considered in the *QoV* suspension performance due to the weight distribution. Figure 10 shows the block diagram of the *SiL* simulation in a *Matlab*[®] environment. The *CarSim*[®] software allows defining all vehicle model parameters as well as the conditions of the simulation test (road roughness, road curvature, driving path, etc).

The *FEB* controller requires knowledge of the main frequency content of the *QoV* motion (Lozoya-Santos et al 2011). In this case this data was estimated as in (Tudon-Martinez et al 2015) using vehicle signals obtained from *CarSim*[®]; only a set variables which would be available in real-world applications were used.

Two sets of *FEB* controllers were tested, one designed using the *Bingham* model and the other with the *ANN* model. In both cases the vehicle dynamics were simulated using

CarSim[®] with the *SO-ANN* model. As shown in section 2.2 the *SO-ANN* model has such a high level of accuracy, both quantitatively and qualitatively, that it can be used as a benchmark of the behavior of the *MR* damper. Note, however, that its complexity currently does not allow controller implementation or adjustment in real-time using low-cost embedded solutions. Therefore, in this article the use of the *SO-ANN* was limited for real-time *QoV* motion simulation using high-power computing platforms.

Three simulation scenarios in *CarSim*[®] were used to compare the suspension performances of both controllers. Each test allows the analysis of the vehicle suspension behavior at a particular road condition:

- (i) A *Bounce Sine Sweep (BSS)* test with decreasing road amplitude (from 0.10 to 0.01 m) with varying frequency

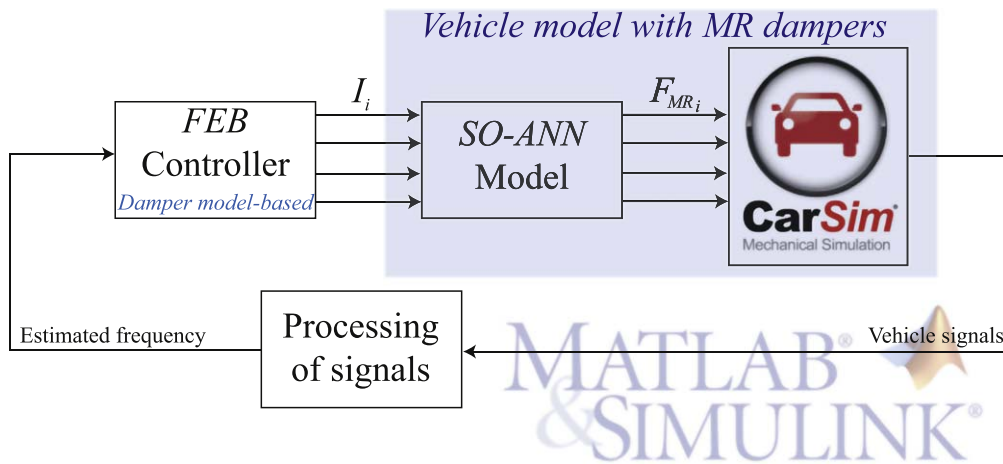


Figure 10. Block diagram of the SiL simulation in Matlab®.

(0.5–12 Hz). In this case the vehicle velocity is maintained at 30 km h^{-1} . This test allows to evaluate the vehicle vertical dynamics at different frequencies, including the resonance frequencies of the chassis ($\sim 2 \text{ Hz}$) and unsprung mass ($\sim 9 \text{ Hz}$).

- (ii) *Three bumps in series* with amplitude of 0.05 m at 30 km h^{-1} without braking. This test quantifies the capacity of the suspension system to reduce the motion when the vehicle is suddenly excited by a bump. In order to excite the roll and pitch motions, the separation between the bumps corresponds to the wheelbase distance whereas the bumps at the right side of the vehicle are out of phase from the ones at the left.
- (iii) An standardized road profile (*type D according to the ISO 8608*) at 50 km h^{-1} . The vertical dynamics are analyzed when the vehicle is driven in a typical situation over a rough road.

Figure 11 shows the transient response of some variables related to the chassis motion and wheel vibrations which can be used to assess the resulting comfort and road holding performances using both controllers. Figure 11 confirms that different control performances in the suspension system are obtained in both cases.

In the *BSS* test, figure 11(a), the vertical acceleration of the chassis is greater from $t = 10$ to $t = 13 \text{ s}$ for the controller based on the *Bingham*-model. This time period is associated with an excitation frequency close to the resonance frequency of the chassis, which is considered as low frequency for this application. The increased vertical acceleration could be related to the inconsistency in the pre-yield zone (associated with lower frequencies) of the *FV* diagram found in the *Bingham* model.

Similarly, figure 11(d) illustrates that the road holding performance is deteriorated with the controller based on the *Bingham* model when operating close to the frequency of resonance of the unsprung mass (around 9 Hz at $t = 20 \text{ s}$). This deterioration could be related to the limited capability of the *Bingham* model to capture the viscous damping phenomenon and its lack of saturation at high frequencies.

In the bumps test (figures 11(b) and (e)), the differences between the two controllers are more difficult to distinguish. Sudden road disturbances complicate the estimation of frequency content; therefore, in this test the performance of the *FEB* controller is being limited by the frequency content estimator rather than by the model quality. That is, model quality has only a slight impact in this test. As expected, figures 11(b) and (e) show almost the same responses for both controllers. After the third bump an increased vertical acceleration and pitch angle are observed when using the controller based on the *Bingham* model. This suggests that up to that point a very similar damper configuration was selected from the lookup table of both controllers. The third bump induced an important threshold crossing for the controller based on the *Bingham* model, which resulted in a significant divergence on the damper configuration of both controllers. This can occur due to numerical issues in the pre-yield zone caused by the discontinuous structure of the *Bingham* model in a simulation environment. Thus, it is clear that the *ANN* model yields a more effective *FEB* controller, even in conditions when the performance of the frequency content estimator is limited.

In the *ISO road profile* test, whose frequency of excitation is around 4 Hz , the magnitude of the vertical heave motion is smaller with the controller based on the *ANN* model, with a reduction of up to 0.01 m , figure 11(c). On the other hand, at 4 Hz the vertical acceleration of the unsprung mass is similar with both controllers, figure 11(f). This result is consistent with the frequency response of the tire deflection shown in figure 7, where an invariant point is located around 4 Hz .

Finally, table 7 shows a quantitative assessment of the suspension performance for both controllers based on the *rms* of the variables plotted in figure 11. The controller based on the *ANN* model has the best comfort and road holding performances with a lower *rms* index in all cases. In particular, using the controller based on the *Bingham* model deteriorates the comfort measurements 11.8% in the *BSS* test, 11.7% in the bumps test and 10% in the road profile test whereas the road holding is deteriorated 48.2% in the *BSS* test, 8% in the bumps test and 0.1% in the road profile test.

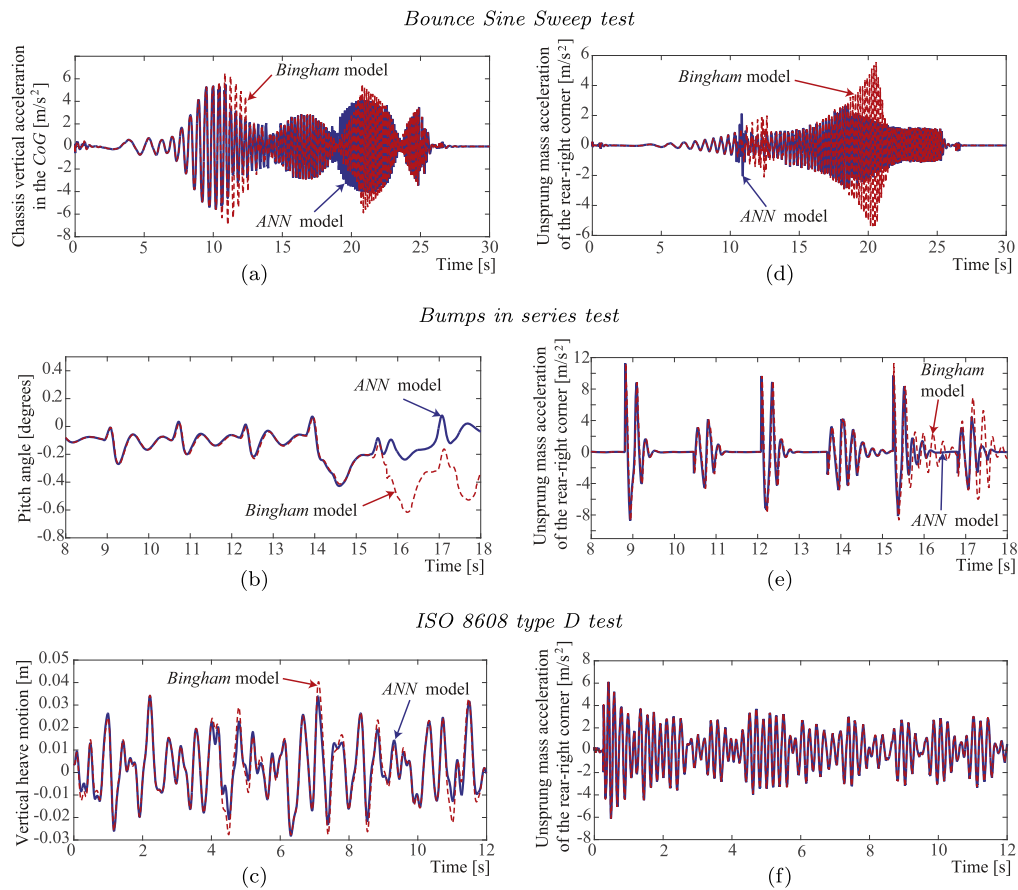


Figure 11. Transient responses of the vehicle in the *SiL* simulation tests, considering the *Bingham* and *ANN* model based controllers: (a)–(c) comfort analysis, (d)–(f) road holding analysis. The four shock absorbers in the *CarSim*[®] vehicle were represented by the *SO-ANN* model.

Table 7. Performance in the transient response of the suspension control systems.

<i>SiL</i> simulation test	Comfort (<i>rms</i> index)		Road holding (<i>rms</i> index)	
	<i>ANN</i>	<i>Bingham</i>	<i>ANN</i>	<i>Bingham</i>
<i>BSS</i>	0.1712 (m s^{-2})	0.1915 (m s^{-2})	0.7288 (m s^{-2})	1.0808 (m s^{-2})
<i>Bumps in series</i>	0.0941 (degrees)	0.1051 (degrees)	1.6306 (m s^{-2})	1.7607 (m s^{-2})
<i>ISO road profile</i>	0.0080 (m)	0.0088 (m)	1.1359 (m s^{-2})	1.1371 (m s^{-2})

According to the aforementioned results, it is notable that the influence of the *MR* damper model used to design the closed loop controllers is easier to perceive in some tests. It is not surprising that the major differences were observed when the vehicle suspension is operating near to its resonance frequencies. In this context, it is important to remember that vehicle velocity and road roughness are the main contributors to the excitation of the suspension system. In a practical application these variables are mostly unknown and difficult to measure. This hinders the possibility of perceiving whether an appropriate *MR* damper model was used for the design of

the suspension control system. As follows some difficulties that can occur by using an inaccurate damper model during the controller design:

- Comfort deterioration around the resonance frequency of the chassis when the stiffness and friction phenomena are not well modeled in the pre-yield region of the *FV* map of the damper (low deflection velocity in the damper).
- Road holding deterioration around the resonance frequency of the unsprung mass when an incorrect linear viscous damping is considered in the post-yield region of the *FV* map of the damper instead of the real nonlinear viscous damping.
- An insufficient damping force when a saturation constraint is not included into the semi-active damper model. That is, the controller may select a lower damping level than the required because an unsaturated model predicts a higher damping level than that actually achieved by the damper.

4.2. Analysis in an experimental *HiL* platform

In this section a further comparison of the controllers designed with the *Bingham* and *ANN* models is presented using a *HiL* setup. This setup allows evaluating the resulting controllers in a more realistic environment subject to noise and other perturbations. This comparative analysis was

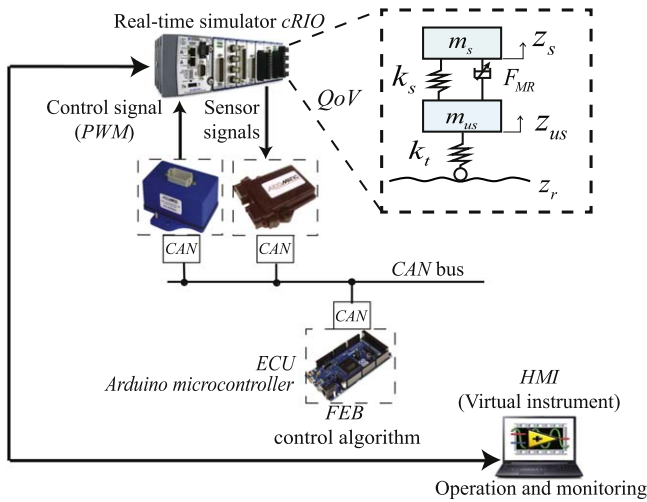


Figure 12. Schematic diagram of the experimental HiL system.

performed in the experimental system depicted in figure 12. The suspension system is composed by a *QoV* model including the *SO-ANN* damper model that is implemented in a *FPGA NI-cRIO* with a sampling frequency of 200 Hz. The *FEB* control algorithm is implemented in a low-cost microcontroller. Both devices, *FPGA* and microcontroller, are communicated through a *CAN* bus.

The *cRIO* chassis includes: (a) an *Analog Output (AO)* module *NI-9263* used to send the *QoV* model outputs to an *Axiomatic Analog Input (AI)* module and (b) a *Digital Input (DI)* module *NI-9426* which receives the *PWM* control signal computed by the microcontroller. The *CAN* network contains an *AX030100 Axiomatic AI* module, an *AX022400 Axiomatic PWM* module and the *Electronic Control Unit (ECU)*, in this case a microcontroller. The *Axiomatic AI* module converts the outputs of the *QoV* model into *CAN* frames. The *ECU* reads the frames of the *Axiomatic AI* module, computes the control signal for the *MR* damper (*SO-ANN* model in *FPGA*) using the *Bingham* or *ANN* model based controller and transmits the control signal through the *CAN* bus. The *Axiomatic PWM* module reads the frames from the *ECU* and generates a *PWM* signal with a duty cycle proportional to the control signal.

4.2.1. Experimental results. Figure 13 shows the frequency response of the closed-loop system when the controller is designed using the *Bingham* and *ANN* models. The test signal consists of a series of 20 independent sinusoidal waves of the form:

$$z_r(t) = R \sin(2\pi f_r t), \quad (7)$$

where $f_r \in [0.5, 1.0, \dots, 11.0]$ is the frequency of the signal in Hz and $R \in [0.10, 0.095, \dots, 0.01]$ is the amplitude in m which decreases inversely to the frequency of motion. For each frequency, 20 cycles have been considered. Thus, $z_r(t)$ represents a chirp signal with decreasing amplitude. Because the suspension (vehicle and damper dynamics) is a nonlinear system, the analysis of the nonlinear frequency response has

been calculated from experimental measurements as follows (Savaresi et al 2010):

- (i) Compute for each variable of interest (including the road input), the discrete *Fourier* transform.
- (ii) Compute the *Power Spectral Density (PSD)* of the variable of interest, denoted as $G_y(f_r)$, and the *PSD* of the road signal, denoted as $G_u(f_r)$.
- (iii) Compute the variance gain $V(f_r)$ at each frequency for each variable of interest, such that

$$V(f_r) = \frac{G_y(f_r)}{G_u(f_r)}. \quad (8)$$

As it was previously discussed in the open-loop frequency response in figure 7, the sprung mass motion performance between 2 and 6 Hz is heavily dependent on the controller action, and consequently on the damper model used for the controller design. In the closed-loop frequency domain analysis, figure 13(a) shows that the *ANN* model based controller yields better comfort performance mainly due to its capacity to represent the viscous damping force in the pre-yield region (low frequency). On the other hand, since the *Bingham* model has a narrower pre-yield zone, the controller based on this model predicts a higher damping force than the real one, resulting in deterioration of comfort performance. For the road holding frequency domain analysis in figure 13(b), the performance between both controllers is similar between 2 and 6 Hz.

To experimentally analyze the transient performance of both controllers, an *ISO 8606 road profile type D* at 60 km h^{-1} was considered in the *HiL* platform. This test is performed to study the suspension dynamics in a typical rough road. Figure 14 shows the experimental transient response of the sprung mass used to monitor the comfort while the unsprung mass displacement is used to analyze the road holding. This test provides a high level of excitation to the suspension dynamics around 4 Hz; therefore, in concordance with the closed-loop frequency response analysis in figure 13(a), the limitations of the *Bingham* model based controller yield a lower comfort performance compared with the *ANN* model based controller. The result is that the *Bingham* model based controller is unable to reduce the sprung mass displacement with the *ISO 8608 road profile* test, figure 14(a).

The road holding performance in this test, as previously observed in the *SiL* simulation test, is practically the same with both controllers, figure 14(b). The reason is the invariant point located around 4 Hz in the unsprung mass frequency response.

4.3. Discussion

The results of both *SiL* and *HiL* studies show that the model used during the controller design has a major effect in the resulting suspension system performance when operating near to the resonance frequency of the sprung and unsprung masses. Although the *Bingham* model is a simple structure

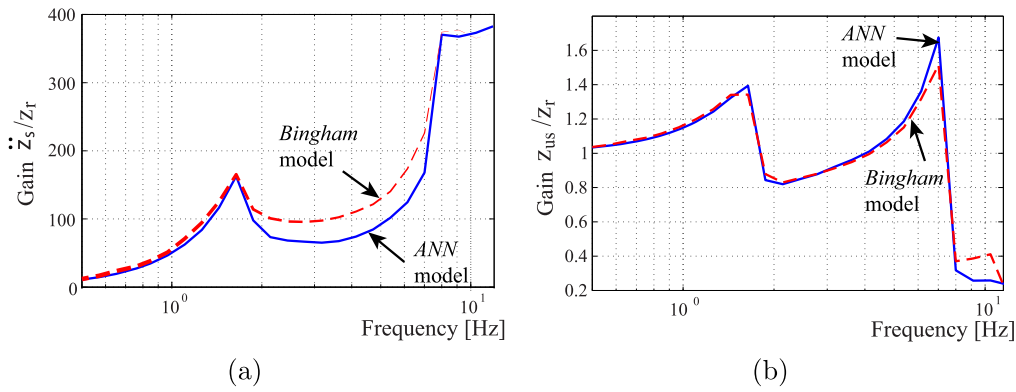


Figure 13. Frequency analysis response of the closed-loop performance in the *HiL* platform, considering the *Bingham* and *ANN* model based controllers for: (a) comfort analysis, (b) road holding analysis. The shock absorber embedded in the *FPGA* device was represented by the *SO-ANN* model.

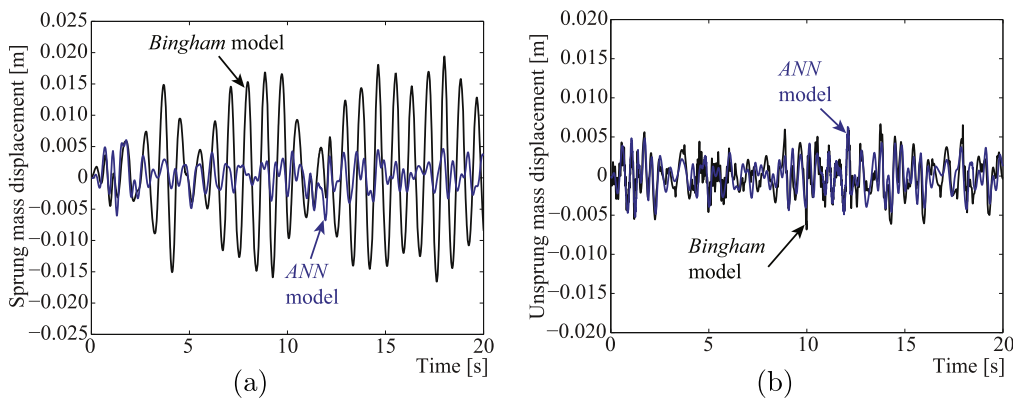


Figure 14. Experimental transient response of the *QoV* in the *HiL* platform, considering the *Bingham* and *ANN* model based controllers: (a) comfort analysis, (b) road holding analysis. The shock absorber embedded in the *FPGA* device was represented by the *SO-ANN* model.

capable of representing linear damped systems accurately, it was shown that using this model for semi-active suspension control design can compromise the vehicle road-holding and comfort properties. Particularly when the road profile has a high-frequency content.

The *SiL* and *HiL* studies show that when the damper model misrepresent the stiffness and friction phenomena in the pre-yield region, the comfort performance can be deteriorated. In addition, the road holding can be affected if the post-yield region is not modeled properly. Finally, the absence of a force saturation constraint at high frequencies in the model can generate inconsistent control actions in this frequency range. Table 8 summarizes the results of both models in terms of their *accuracy* to represent the *MR* damper nonlinearities and *effectiveness* for a control application. *BSS* test in *SiL* explores all main nonlinear *MR* phenomena in the whole *FB* of interest, showing that the *Bingham* model cannot represent properly the dynamics in the pre-yield and post-yield stress zone. Thus, the *ANN* model is more effective for a suspension controller design at these conditions. *Bumps* test in *SiL* only explores *MR* phenomena at very low frequencies. In this operating region both models are accurate; therefore, both models are effective for control design purposes. The differences that may appear in

simulations are mostly numerical issues due to the discontinuity in the *Bingham* model. For the *ISO road* profile tests (*SiL* or *HiL*), model accuracy depends on the road roughness and vehicle velocity. For instance, in rough roads at low vehicle velocity lower operating frequencies are present. In this condition both models are accurate enough to represent the *MR* phenomena; therefore, both models are effective in a suspension control application at these conditions. However, at higher vehicle velocities (higher operating frequencies) the *Bingham* model cannot reproduce the hysteresis and saturation properly. Thus, in this case the *ANN* model is recommended for the suspension controller design.

As final remark is that the performance deterioration observed when using the least accurate model can be mis-handled by the engineers in charge of the implementation of the suspension system. In particular, instead of improving the quality of the damper model, the following unnecessary actions are common:

- (i) Time-consuming tuning of the controller parameters via trial and error.
- (ii) Use of more conservative controllers.
- (iii) Change of control strategy.

Table 8. Analysis of the *model accuracy* and its relation to the *model effectiveness* for a suspension control application.

Test		Model accuracy					Model effectiveness		Application	
		Pre-yield zone		Post-yield zone		Saturation	Relative suspension performance			
		Stiffness	Friction	Hysteresis	NL damping		Comfort	Road-holding		
<i>SiL</i>	<i>BSS</i>	ANN ✓ Bingham ×	ANN ✓ Bingham ✓	ANN ✓ Bingham ×	ANN ✓ Bingham ×	ANN ✓ Bingham ×	11.8% ↑ with ANN	48.2% ↑ with ANN	Sportive	ANN
	<i>Bumps</i>	ANN ✓ Bingham ✓	ANN ✓ Bingham ✓				11.7% ↑ with ANN	8% ↑ with ANN	Urban	Both
	<i>ISO road</i>	ANN ✓ Bingham ×	ANN ✓ Bingham ✓	ANN ✓ Bingham ×	ANN ✓ Bingham ✓	ANN ✓ Bingham ×	10% ↑ with ANN	0.1% ↑ with ANN	Urban	Both
<i>HiL</i>	<i>ISO road</i>	ANN ✓ Bingham ×	ANN ✓ Bingham ✓	ANN ✓ Bingham ×	ANN ✓ Bingham ✓	ANN ✓ Bingham ×	45.9% ↑ with ANN	1.3% ↑ with ANN	Urban	ANN

5. Conclusions

For model-based control, model accuracy is a key element in order to achieve high-performance levels. In this context, the accuracy of a particular model can be appreciated differently depending on the application. Therefore, the concept of *model effectiveness* is introduced in this article; that is, a model whose properties render it useful for a particular task. In this context, *MR* dampers comprise several physical phenomena and interactions which can be modeled with different degrees of accuracy, each one distinctly contributing to the effectiveness for particular applications.

This article studied the relationship between specific *MR* damper model properties and the resulting effectiveness for control design. In order to achieve this goal three damper models were obtained from experimental data. First, for controller design purposes, an *ANN* based model (*MLP*) and, (b) the well known *Bingham* model were obtained. A third model, based on a more complex *ANN* architecture using recurrent networks, was also obtained for simulation and benchmarking purposes; this representation is denoted here as a *Simulated Oriented-ANN (SO-ANN)* model. In this context, the main idea of this paper is to present the effects that can occur in the closed-loop performance of an automotive suspension system when the model is unable to represent relevant nonlinear *MR* phenomena. For this case of study, the *ANN* and *Bingham* models were chosen because of their different nonlinear modeling features.

The differences among the models were studied both qualitatively and quantitatively. The main qualitative differences between the *Bingham* and simple *ANN* models were found to be the pre/post yield behaviors as well as the force saturation. These differences were effectively captured by some quantitative measurements; however, it should be observed that it is not easy to determine how a particular qualitative model limitation will reflect into the actual quantitative error. This is true particularly after considering that quantitative modeling error shows a large range of variation among different tests. This suggests that specific tests could be used to identify specific qualitative limitations, but this has not been currently studied for *MR* dampers in a control design context. Therefore, a wide range of tests is still suggested (Lozoya-Santos *et al* 2012).

After the model assessment, a control approach which is applicable to both control-oriented models is used to design a *FEB* controller. This control strategy allows extracting all the relevant frequency domain information contained in the design models, which has been shown to be the main aspect which defines the dynamics of suspension systems. The resulting controllers (one based on the *Bingham* model and other on *ANN*) are then implemented in (a) a *SiL* by using *CarSim*[®] with *Matlab Simulink*[®] and (b) a *HiL* by using a real-time module based on a *FPGA*, *CAN* communication and a low cost microcontroller. The first configuration allows to evaluate the effect of the full car dynamics in the resulting suspension control system while the *HiL* setup allows introducing noise and perturbations into the control loop as well as evaluating the feasibility of the implementation of the studied

control strategy in low-cost embedded solutions, which is in line with typical automotive control applications.

The results of the study revealed that *MR* damper model effectiveness for controller design is affected mainly by its properties around the chassis and unsprung masses resonance frequencies. In fact, when a controller based on the *Bingham* model is used the suspension performance can be severely compromised if the vehicle is operated with a road profile with high frequency content around the aforementioned frequencies.

As a summary, the major factors that limit the effectiveness of an *MR* damper model for automotive suspension control design are:

- (i) When the damper model lacks the capacity to represent the stiffness and friction phenomena in the pre-yield region (low frequencies in the *FV* diagram of the damper).
- (ii) When the post-yield region is wrongly represented by a linear viscous damping function.
- (iii) When the damping force is not saturated at high velocities.

Each of the aforementioned cases compromises the suspension performance in a particular manner and should be avoided at the modeling stage in order to avoid unnecessary and time-consuming effort at later stages of the control design and implementation.

Funding

Authors thank CONACyT for the partial support in this research and METALSA for sharing its experimental setup.

ORCID iDs

Juan C Tudon-Martinez  <https://orcid.org/0000-0003-0646-1871>

Diana Hernandez-Alcantara  <https://orcid.org/0000-0003-0598-702X>

Jorge de J Lozoya-Santos  <https://orcid.org/0000-0001-5536-1426>

References

- Boada M, Calvo J, Boada B and Díaz V 2011 Modeling of a magnetorheological damper by recursive lazy learning *Int. J. Non-Linear Mech.* **46** 479–85
- Çesmeçi S and Engin T 2010 Modeling and testing of a field-controllable magnetorheological fluid damper *Int. J. Mech. Sci.* **52** 1036–46
- Chadli M, Hajjaji A and Rabhi A 2010 H_∞ observer-based robust multiple controller design for vehicle lateral dynamics *American Control Conf.* pp 1508–13
- Chang C and Zhou L 2002 Neural network emulation of inverse dynamics for a magnetorheological damper *J. Struct. Eng.* **128** 231–9

- Chen E, Si C, Yan M and Ma B 2009 Dynamic characteristics identification of magnetic rheological damper based on neural network *Artificial Intelligence and Computational Intelligence* (China: IEEE Computer Society) pp 525–9
- Choi S, Lee S and Park Y 2001 A hysteresis model for field-dependent damping force of a magnetorheological damper *J. Sound Vib.* **245** 375–83
- Choi S B, Lee H S and Park Y P 2002 H_∞ control performance of a full-vehicle suspension featuring magnetorheological dampers *Veh. Syst. Dyn.* **38** 341–60
- Dixon J 2007 *The Shock Absorber Handbook* 2nd edn (New York: Wiley)
- Do A, Senname O and Dugard L 2012 LPV modelling and control of semi-active dampers in automotive systems *Control of Linear Parameter Varying Systems with Applications* (Berlin: Springer) ch 5 (https://doi.org/10.1007/978-1-4614-1833-7_15)
- Du H, Lam J and Zhang N 2006 Modelling of a magneto-rheological damper by evolving radial basis function networks *Eng. Appl. Artif. Intell.* **19** 869–81
- Du H, Szeb K and Lam J 2005 Semiactive H_∞ control of vehicle suspension with magneto-rheological dampers *J. Sound Vib.* **283** 981–96
- Dutta S and Chakraborty G 2014 Performance analysis of nonlinear vibration isolator with magneto-rheological damper *J. Sound Vib.* **333** 5097–114
- Dutta S and Chakraborty G 2015 Modeling and characterization of a magneto-rheological fluid based damper and analysis of vibration isolation with the damper operating in passive model *J. Sound Vib.* **353** 96–118
- Fijalkowski B 2011 *Automotive Mechatronics: Operational and Practical Issues* vol 2 (Berlin: Springer) (<https://doi.org/10.1007/978-94-007-0409-1>)
- Guo D, Hu H and Yi J 2004 Neural network control for a semi-active vehicle suspension with a magnetorheological damper *J. Vib. Control* **10** 461–71
- Guo S, Yang S and Pan C 2006 Dynamical modeling of magneto-rheological damper behaviors *J. Intell. Mater., Syst. Struct.* **17** 3–14
- Hong K, Sohn H and Hedrick J 2002 Modified skyhook control of semi-active suspensions: a new model, gain scheduling, and hardware-in-the-loop tuning *ASME Trans. J. Dyn. Syst. Meas., Control* **124** 158–67
- Imaduddin F, Mazlan S, Ubaidillah I M and Bahiuddin I 2017 Characterization and modeling of a new magnetorheological damper with meandering type valve using neuro-fuzzy *J. King Saud Univ.—Sci.* **29** 468–77
- Karnopp D, Crosby M and Harwood R 1974 Vibration control using semi-active force generators *J. Eng. Ind.* **96** 619–26
- Kwok N, Ha Q, Nguyen T, Li J and Samali B 2006 A novel hysteretic model for magnetorheological fluid dampers and parameter identification using particle swarm optimization *Sensors Actuators A* **132** 441–51
- Lozoya-Santos J, Morales-Menendez R, Ramírez-Mendoza R, Tudón-Martínez J, Senname O and Dugard L 2012 Magnetorheological damper—an experimental study *J. Intell. Mater. Syst. Struct.* **23** 1213–32
- Lozoya-Santos J, Morales-Menendez R, Senname O, Dugard L, Ramírez-Mendoza R and Tudón-Martínez J 2011 Control strategies for an automotive suspension with a MR damper *18th IFAC World Congress* pp 1820–5
- Metered H, Bonello P and Oyadji S 2010 The experimental identification of magnetorheological dampers and evaluation of their controllers *Mech. Syst. Sig. Process.* **24** 976–94
- Poussot-Vassal C, Senname O, Dugard L, Gáspár P, Szabó Z and Bokor J 2008 A new semi-active suspension control strategy through LPV technique *Control Eng. Pract.* **16** 1519–34
- Poussot-Vassal C, Spelta C, Senname O, Savaresi S and Dugard L 2012 Survey and performance evaluation on some automotive semi-active suspension control methods: a comparative study on a single-corner model *Annu. Rev. Control* **36** 148–60
- Prabakar R, Sujatha C and Narayanan S 2014 Response of a half-car model with optimal magneto-rheological damper parameters *J. Vib. Control* **22** 784–98
- Şahin I, Engin T and Çeşmeci Ş 2010 Comparison of some existing parametric models for magnetorheological fluid dampers *Smart Mater. Struct.* **19** 035012
- Sandu C, Southward S and Richards R 2010 Comparison of linear, nonlinear, hysteretic, and probabilistic models for magnetorheological fluid dampers *ASME J. Dyn. Syst., Meas., Control* **132** 061403
- Savaresi S, Bittanti S and Montiglio M 2005 Identification of semi-physical and black-box non-linear models: the case of MR-dampers for vehicles control *Automatica* **41** 113–27
- Savaresi S, Poussot-Vassal C, Spelta C, Senname O and Dugard L 2010 *Semi-Active Suspension Control for Vehicles* (Oxford: Elsevier) (<https://doi.org/10.1016/C2009-0-63839-3>)
- Singru P, Raizada A, Krishnakumar V, Garg A, Tai K and Raj V 2017 Modeling of a magneto-rheological (MR) damper using genetic programming *J. Vibroeng.* **19** 3169–77
- Song X, Ahmadian M and Southward S 2005 Modeling magnetorheological dampers with application of nonparametric approach *J. Intell. Mater. Syst. Struct.* **16** 421–32
- Spencer B, Dyke S, Sain M and Carlson J 1996 Phenomenological model of a MR damper *ASCE J. Eng. Mech.* **123** 230–8
- Stanway R, Sproston J L and Stevens N G 1987 Non-linear modeling of an electro-rheological vibration damper *J. Electrost.* **20** 167–84
- Tang X, Du H, Sun S, Ning D, Xing Z and Li W 2017 Takagi-sugeno fuzzy control for semi-active vehicle suspension with a magnetorheological damper and experimental validation *IEEE/ASME Trans. Mechatronics* **22** 291–300
- Tudon-Martinez J, Fergani S, Senname O, Martinez J, Morales-Menendez R and Dugard L 2015 Adaptive road profile estimation in semiactive cars suspensions *IEEE Trans. Control Syst. Technol.* **23** 2293–305
- Tudón-Martínez J, Lozoya-Santos J, Morales-Menendez R and Ramírez-Mendoza R 2012 An experimental artificial-neural-network-based modeling of magneto-rheological fluid dampers *Smart Mater. Struct.* **21** 1–16
- Tudon-Martinez J, Vivas-Lopez C, Hernandez-Alcantara D, Morales-Menendez R, Senname O and Ramirez-Mendoza R 2018 Full vehicle combinatory efficient damping controller: experimental implementation *IEEE/ASME Trans. Mechatronics* **23** 377–88
- Valasek M, Novak M, Sika Z and Vaculin O 1997 Extended ground-hook—new concept of semi-active control of truck's suspension *Veh. Syst. Dyn.* **27** 289–303
- Wang H and Song G 2011 Fault detection and fault tolerant control of a smart base isolation system with magneto-rheological damper *Smart Mater. Struct.* **20** 1–9
- Wang J, Wilson D, Xu W and Crolla D 2005 Active suspension control to improve vehicle ride and steady-state handling *44th IEEE Conf. on Decision and Control and the European Control Conf.* pp 1982–7
- Waubke H and Kasess C H 2016 Gaussian closure technique applied to the hysteretic bouc model with non-zero mean white noise excitation *J. Sound Vib.* **382** 258–73
- Werely N, Pang L and Kamath G 1998 Idealized hysteresis modeling of electrorheological and magnetorheological dampers *J. Intell. Mater. Syst. Struct.* **9** 642–9
- Yang G, Spencer B and Dyke S 2002 Large-scale MR fluid dampers: modeling and dynamic performance considerations *Eng. Struct.* **24** 309–23
- Zapateiro M, Luo N, Karimi H and Vehí J 2009 Vibration control of a class of semiactive suspension system using neural network and backstepping techniques *Mech. Syst. Sig. Process.* **23** 1946–53